A demonstration of the mechanical sensing capability of individually contacted vertical piezoelectric nanowires arranged in matrices

Mitesh Parmar, Edgar A.A. Leon Perez, Gustavo Ardila, Elise Saoutieff, Emmanuelle Pauliac-Vaujour, Mireille Mouis

A demonstration of the mechanical sensing capability of individually contacted vertical piezoelectric nanowires arranged in matrices

Mitesh Parmar[a*+], Edgar A. A. Leon Perez[ab*++], Gustavo Ardila[a], Elise Saoutieff[b], Emmanuelle Pauliac-Vaujour[b] and Mireille Mouis[a]

[a] Univ. Grenoble Alpes, CNRS, Grenoble INP, IMEP-LaHC, F-38000 Grenoble, France

[b] Univ. Grenoble Alpes, CEA, Leti, DSYS, F-38000 Grenoble, France

Corresponding Author: Gustavo Ardila (ardilarg@minatec.grenoble-inp.fr); Elise Saoutieff (elise.saoutieff@cea.fr)

* These authors contributed equally to this article.
+ Present adress : INL – International Iberian Nanotechnology Laboratory, Avenida Mestre José Veiga, 4715-330 Braga, Portugal
++ Present adress : STMicroelectronics (Crolles 2) SAS, 850 Rue Jean Monnet, 38926 Crolles CEDEX, France

Abstract

This paper reports the fabrication of arrays of vertical piezoelectric nanowires which are individually contacted at their base, and demonstrates that an electrical response to strain can be obtained from individual nanowires from the array, without external biasing exploiting the piezotronic effect. Such a technology could thus be used for the fabrication of self-powered sensors for mechanical strain mapping, where each individually contacted nanowire would act as the strain sensing equivalent of a pixel. Lateral mapping resolutions in the micrometer range can be obtained. Here, the hydrothermal method was used to grow vertical ZnO nanowires selectively between two electrodes that had been patterned beforehand. For the sake of demonstration, nanowires deflection was produced by subjecting the array of nanowires to an incident lateral gas flow of controlled rate, which was switched on and off repeatedly across the sample while electrical response was measured. Different experimental configurations were tested in terms of flow rate, flow orientation, or nanowire position with respect to tube outlet. Experiments were carried out with compressed nitrogen and air. The experimental results are fully consistent with the piezoelectric and piezotronic response which can be expected with this geometry. Moreover, it is shown that the electrical response under nitrogen flow is a linear function of flow rate and that its sign provides information about flow direction. These results demonstrate the very promising prospects of this new technology for high-resolution mapping, with potential applications in gas or liquid flow sensing, fingerprints detection or human-machine interfaces.

Keywords — **Mechanical sensor, Microfabrication; Piezotronics, ZnO nanowires, Strain mapping**

1. Introduction

Nanosized objects have demonstrated manifold advantages when it comes to designing devices with extreme characteristics and performances in domains such as sensors, optoelectronics or piezotronics [1, 2, 3]. In particular, the viability of lateral [4, 5] and vertical piezoelectric nanowires (NWs) for sensor applications has already been investigated and demonstrated [6, 7, 8]. The advantage of using vertical nanowires is related to the possibility to reach high integration densities and to the leveraging effect of the vertical nanowire geometry under bending. Indeed, some non-centrosymmetric crystals such as ZnO [9] and GaN [10, 11] can be heterogeneously integrated into nanoelectronics devices [7] in the shape of highly elastic one-dimensional nanostructures [12], giving access to a full range of unprecedented sensitivities and resolutions.

Vertically integrated NWs (also called VING for Vertically Integrated Nanogenerators) have been extensively studied for energy harvesting applications [13, 14, 15], mechanical sensors [16, 17], gas sensor [18] as well as ultrasound/sound detector [19, 20]. ZnO NW vertical arrays have been used as well for tactile imaging exploiting the piezotronic effect [9]. These vertically integrated NWs reported-works employ different phenomenon such as piezoelectric and/or piezotronics - which is an accumulative effect of the piezoelectric as well as the semiconducting nature of the material [3]. In piezotronics, when the NWs are electrically contacted creating Schottky junctions, the piezopotential generated due to the applied strain further modulates the Schottky barrier height and thus varies the current flowing through the device when an external bias is applied.

In most of the above-mentioned publications, nanowires have been actuated collectively. The capability of individual piezoelectric semiconducting NWs as mechanical sensors has been also studied by different techniques and configurations: (i) In the very first report of the mechanical sensing capability of ZnO individual NWs, an AFM tip was used to

bend or compress the NWs in order to generate a piezopotential [6], in other reports, a bias was applied as well at the AFM tip, thus exploiting the piezotronic effect [10, 11, 21, 22]. In these techniques, the NW was electrically contacted with one electrode at its base (very often the substrate) and the second electrode was provided by the AFM tip. (ii) Other reports consisted in the vertical [23] or lateral [24] integration of single NWs electrically connected at both ends. In these cases, the piezotronic effect is mostly exploited as well by fabricating a piezotronic transistor. Here, the piezopotential produced under an applied strain, act as gate potential for the transistor operation.

Concerning the vertical integration of NWs into devices, most of the studies do not concern the lateral resolution but rather use large electrodes intended at getting larger energy. However, this configuration can also be used to fabricate sensing arrays with high lateral resolution. An example of such implementation has been demonstrated, using single or a bundle of NWs grown over individual electrodes, covered by a polymer and then with a top collective electrode [25, 26] (See Fig. 1a)

In contrast, the electrodes can also be positioned at the bottom of the nanowire, where the piezoelectric response to a bending of the nanowire has been shown to be maximum [27], so as to provide high sensitivity to lateral deflections. Such configuration has been implemented using the selective growth of vertical NWs between two electrodes positioned at their base. (See Fig. 1b) This second technology, although more challenging, is expected to provide higher resolution with a minimal volume [28].

In this paper, we investigated the piezotronic response of such piezoelectric semiconducting vertical NWs individually contacted on two sides at their bottom. The fabrication technology that was developed allows them to be arranged in matrices, with the aim of getting the strain equivalent of a pixel with each individually contacted nanowire. Device design of the unit sensor and optimization were anticipated through microfabrication-guided

finite element simulations [8, 27].

As can be seen in Fig. 1c, Electrodes are placed at the bottom of the structure where the maximum potential difference is expected to be generated under bending from FEM simulations considering only the piezoelectric effect and no semiconducting properties [27]. A lateral bending will generate a piezoelectric potential affecting the Schottky barrier heights at both electrodes, thus a variation of the current can be detected (See Fig. S1 in the supporting material). [29, 30]

Crystalline ZnO NWs were chosen on the basis of their excellent inherent material properties, including non-toxicity and biocompatibility, besides their intrinsic piezoelectric properties, with no need for preliminary poling step [31, 32]. Moreover, it has been shown that the association of a thin nanowire geometry to the presence of slow traps and Fermi level pinning at the surface of ZnO could reduce the technological constraints on residual doping, so that, for usual experimental doping levels, piezoelectric coefficients of nanowires could be enhanced compared to those of bulk material, thereby improving the limit of detection as strain sensor [14, 33].

The main challenge in the development of vertically aligned single-NW-based sensor arrays is to integrate an array of individual ZnO NWs over microelectronic chips, while considering process compatibility at the wafer scale. Section II presents the specific microfabrication clean-room process that was developed to ensure controlled NW positioning at specific locations on the processed chips and contact alignment at nanowire bases. ZnO NWs were grown by using the hydrothermal growth as described in our previous published work [14, 34]. The control of NWs positions was obtained by a combination of hard-masking and the optimization of selective growth conditions. Finally, the alignment between metal contact lines and hard-mask openings for NW growth was achieved by a combination of UV and e-beam lithography and several levels of metal contacts in order to fabricate elementary devices

[35]. As described in section III, a specific characterization set-up was developed to test mechanical sensing capability. The bending of individual NWs was exerted and relieved by the switching of a controlled gas flow while electrical response was measured under different experimental conditions. Experimental results are presented and discussed in Section IV. In particular, they demonstrate a highly linear and flow orientation dependent response as a function of flow rate which is very promising for sensing applications. These results show prospects of this new technology for high-resolution mapping for applications in gas or liquid flow sensing [36], fingerprints detection [29] or human-machine interfaces [37].

2. Fabrication

2.1. Device architecture

The architecture consists of individually contacted piezoelectric NWs, vertically grown between two electrodes on silicon substrate. Device schematics is described in Fig. 2.

The elementary sensing pixel considered in this work was made up of a silicon substrate (111), a gallium-doped ZnO seed-layer, one vertical ZnO NW grown from the seed layer and two gold metallic electrodes, insulated from the ZnO seed layer, and placed at the NW base. The fabrication technology involved the fabrication of several matrices of such elementary sensing pixels.

2.2. Localized nanowires growth:

Fig. 3 illustrates the successive technological steps towards selective growth of ZnO NWs matrices by hydrothermal growth method. As described in the process flow, the process starts with chemical vapor deposition (CVD) of a gallium doped seed layer. A hard mask technique was used to expose locally this seed layer during hydrothermal growth, thus promoting localized nanowire growth and controlled NW positioning above the chip.

ZnO NWs were synthesized by hydrothermal growth method on top of 50 nm thick ZnO doped with gallium seed layer deposited by CVD over Si(111) substrate. A careful optimization of growth conditions and opening dimensions was carried out to ensure selectivity, with no ZnO nucleation outside the openings and good control of the number of nanowires grown in each opening. In brief, the growth solution was prepared with zinc nitrate hexahydrate ($Zn(NO_3)_2 \cdot 6H_2O$) and hexamethylenetetramine (HMTA) precursors in equimolar concentration (10 mM), growth time of 5h and growth temperature of 90°C [38, 39]. The resulting process is low cost, easily scalable and its low temperature makes it compatible with integration on most electronic components as well as on organic materials.

The density of NWs array for the intended application of mechanical strain mapping is an important factor to consider. The density of the array depends on the nucleation which worked as starting point of the growth. The nucleation density is further influenced by the precursor concentrations, growth temperature, growth time and seed layer morphology.

Another way to control the density of NWs array is to control the exposed area of the seed layer at each pixel position. At this stage, a Si_3N_4 hard mask approach was preferred to resist patterning as it offers the three-fold advantages of a higher pattern resolution, the ability to withstand physical as well as chemical process steps and the opportunity of depositing and patterning the electrodes prior to NW growth. However, it also affects the electrical output as the potential is generated by the sole NW without contribution of the seed layer. Moreover, there will be a capacitive effect in case the electrical connection between the NWs and the electrode is lost [27].

As discussed before, a Si_3N_4 hard mask was employed to selectively control NW positions. This hard mask was open in two steps, with a partial opening before metal deposition, followed by full opening to expose the seed layer before NWs growth. This strategy ensured that the seed layer was protected from the solvents and resists used for metal deposition.

As NWs growth by hydrothermal method is mass transport limited [40], growth conditions, openings size and distance between openings had to be optimized in order to reach the target array arrangement with one single nanowire per pixel. The size of each opening to the underlying ZnO seed layer was experimentally optimized by varying its diameter from 100nm to 1000 nm. The openings were arranged according to the lattice pattern shown in Fig. 4a. After pixel-area optimization, the optimum was found with 150 nm wide openings separated by 2000 nm distance. The patterns were defined by e-beam lithography and dry-etching (ICP-RIE etching) through a 100nm-thick Si_3N_4 layer deposited on top of the ZnO seed-layer.

These values were found to lead to isolated NWs on most of the openings of the hard-mask as seen in Fig. 4b and Fig. 4c. NWs have an average length and diameter of 2393 ± 104 nm and 372 ± 59, respectively.

It was observed that there can be more than one nucleation resulting in multiple NWs per opening. As precursor concentration influences nucleation for the growth of NWs, the process still needs optimization in order to obtain one single NW per exposed area. This is possible and been reported in the literature although using bulk c-plane ZnO single crystals as substrates [41]. In the present work, only single NW based samples were exploited for the use of mechanical sensing.

2.3. Fabrication of mechanical sensor

In order to obtain the sensor configuration of Fig. 2, and before the NWs growth described previously, contact alignment between metallic lines and hard-mask openings for nanowire growth was achieved using a combination of UV and e-beam lithography and several levels of metal contacts (see Fig. 5(a)–(d)). Selective NW growth yielded ZnO NWs with a

length that could be varied between 1µm to 2 µm and maximum diameter of about 400 nm for the opening's configuration described above (see Fig. 5(e) and (f)).

The above described process is a collective process where several sensors are processed at the same time on the chip. In this experiment, we worked on 10 mm x 10 mm chips. With the planar interconnect routing used here, it was not possible to contact all the nanowires from the array. Only 10 of them could be contacted so that each sensing device comprised 10 pixels, each connected to 2 output pads. Fig. 5(a) shows a top-view of 9 devices sensing devices from the same chip, while Fig. 5(b) zooms on one single device with its 20 metallic output pads (50 µm x 50 µm) connected to 5 µm wide metal lines. Fig. 5(c) zooms further on the central area of the device where the 5 µm-wide metal lines contact smaller pads (5 µm x 5 µm), which are connected to narrower metal lines of 250 nm width. These narrower lines were aligned to the hard-mask openings for the NW growth as shown in Fig. 5(d). Examples of final device after nanowire growth are displayed on Fig. 5(e) and (f), with 2 different degrees of magnification. No short-circuits between adjacent NWs and metallic lines were observed.

3. Characterization of individual sensor pixels

The lateral deflection of NWs was produced by a controlled incident gas flow and the electrical response was measured (See Fig. 6a). During the analysis, the samples were fixed on the chuck using vacuum. The controlled gas flow was directed to the sample through a 10 mm diameter plastic tube placed at the distance of 5 mm away from the sample. The tube was fixed in order to restrict its movement during the analysis. The complete characterization set-up can be seen in Fig. S2 in the supporting material. It consists of a Karl Suss PM8 Probe station, a Semiconductor analyzer (HP 4155A), a Digital oscilloscope and function generator as well as a gas source connected with Digital mass flow controller (MFC) – Horiba SEC-N100. The gas flow rate is measured in Standard Liter per Minute (SLM). The MFC have a flow rate at the outlet in the range 0-10 SLM. In this work a gas rate in the range of 0 to 6 SLM was used. We

used both compressed air and compressed nitrogen, with a pressure fixed at 1 bar using the output pressure regulator. The function generator regulated gas flow by providing a square voltage signal to the MFC. The output signal of the MFC can be viewed in the oscilloscope (See Fig. S2). The impact of gas flow on the NWs generated an output current variation (see next section). Current variation was recorded in real time using the semiconductor analyzer.

4. Results and discussions

The electrical characteristic analyses of the mechanical sensor were carried out in two stages on two samples (sample #1 and sample #2). Firstly, the quality of the electrical contact between the electrodes and the nanowires was verified by testing the current-voltage (I-V) characteristics of the device (refer to the supporting material for further details). The characterization of the electrical response of the device to nanowire bending was then carried out, to test the device in its sensing mode, both electrodes and the substrate were grounded and the current measured at the first contact (C1) as depicted in Fig. 6b and Fig. 6c. This does not mean however that there is no voltage difference between the contacts, as many parasitic effects can produce a small voltage which is enough to drive a small current through the device.

In this mode, the gas flow was used to bend the nanowires. It is then expected from the theory [27][29] that the strain generated at the bottom of the nanowire results in a piezoelectric potential, and by the piezotronic effect, a Schottky barrier height variation, thus a conduction current variation. The experimental set-up was used to measure the time variation of the current that flew through the semiconductor analyser while the flow was switched ON and OFF repeatedly with a controlled flow rate. The experiment was carried out using nitrogen (N_2) or air.

Fig. 7(a) shows the typical time-dependent electrical response with N_2 gas-flow switched between 0 SLM and 4 SLM. While the gas-flow was controlled using a square-wave with 20 sec cycling period, the sensor responded accordingly. The output characteristics of the

mechanical sensor at different flow rate can be seen in Fig. 7(b) where the current variation increases with the increase of flow rate. The value of the current at the OFF state is a reference to measure the current variation of the sensor under bending, but this value is not controlled at this stage and can be influenced by many parameters (i.e. calibration of the semiconductor parameter, contact quality between the probes and the electrodes, asymmetries in the device, light exposure, etc.)

Initially, the sensing analysis was done using nitrogen (N_2) gas (a comparison of the response of both samples #1 and sample #2 can be seen in Fig. S5 in the supplementary material). Fig. 7c and Fig.7d further compares the sensor response obtained with nitrogen and air. Here, Fig. 7c shows the sensor response for N_2 gas flow whereas the sensor response during air flow is plotted in Fig. 7d. As can be observed, the response is linear when using N_2 but this characteristic is lost when with air. The electrical response of the sensor was about 5 times higher with N_2 gas than with air in the same range of gas flow. This might be due to the presence of oxygen in the compressed-air flow. Indeed, oxygen is known to interact with the surface of ZnO [42], possibly modifying the electronic states at the surface of the nanowires creating a depletion region in the NW. Such a modification of surface states could affect the piezoelectric response [33]. The effect of air and oxygen in ZnO NW based devices have been reported in experiments as well [18, 43], in particular, a nanogenerator performance under compression was increased (more potential generated) when exposed to a higher concentration of Oxygen [18]. However, in the applications foreseen for our device, we want to reduce this effect. However, it has been shown that ZnO nanowires could be protected from such effect by means of a thin alumina passivation layer [44]. This could provide a solution to this issue.

The dependence of individual sensor response with flux orientation has been analyzed by changing the orientation of the sample with respect to gas tube outlet. As can be seen in the Fig. 8, there was a clear difference in the direction of current variation with the orientation of

the device. For normal orientation (Fig. 8a), the current varied in the positive direction where as for the reverse orientation, the current variation was in the negative direction, as expected from the piezoelectric theory (Fig. 8b). Fig. 8c further shows the electrical response of the individual sensor as a function of flow rate for 3 different orientations with respect to gas tube outlet: normal, reverse and perpendicular. This response was measured by the amplitude of the current difference between ON and OFF gas flow. Consistently with what could be expected theoretically, the response was positive for normal orientation, negative for reverse orientation and close to zero for perpendicular orientation. The latter result was expected as the strain was perpendicular to the axis of the electrodes and gives another confirmation that the device is indeed detecting the piezoelectric response correctly. In all three cases, the response is very linear with flow rate. To our knowledge, this is the first time that such clear result is shown.

In order to analyze the results further, it is necessary to account for the fact that the distance of the nanowire under test with respect to tube outlet was modified as the sample orientation was changed. Therefore, it is expected that the pressure applied by the gas on the nanowire varies not only in direction, but also in intensity while the sample is turned. The nanowire under test was close to the edge of the chip, thus close to tube outlet with “normal” orientation. Conversely, its distance to tube outlet was strongly increased with “reverse” orientation. For the perpendicular orientation, the absence of response was expected as the electrodes were then placed at positions where the piezoelectric potential was identical on both sides of the nanowire. The small residual signal measured could be either due to the broadening of the gas flow or to a small misorientation of the chip, due to manual handling. As a whole, the measured response was thus (i) maximal as the nanowire was closer to the tube outlet, (ii) opposite when the bending was reversed and strongly decreased in absolute value while the distance to the tube outlet was increased, and (iii) almost null when the bending was normal to the axis of the electrodes. Although more quantitative measurements should be carried out to

transform these observations into calibrated results, the observed variation of the electrical response of our individually contacted nanowires can thus be interpreted as an indication that the device is able to map the local variations of flow, both in amplitude and direction.

5. Conclusions and perspectives

The present work aimed at bringing the proof-of-concept of self- powered mechanical sensors based on vertical ZnO nanowires exploiting the piezoelectric effect. We developed a scalable technology, able to provide matrices of individual sensors. Each of them consisted in one nanowire with 2 contacts at its base. To do so, ZnO NWs were selectively grown by hydrothermal process over patterned electrodes. For this initial demonstration, a bending force was exerted on the nanowires and relieved repeatedly by switching a controlled gas flow on and off. Several important experimental results were obtained from the response of a single sensor. A linear response with flow rate was obtained for all the tested orientations when nitrogen was used. We suspect that the documented influence of oxygen on ZnO interferes with the piezoelectric phenomena when air was used. The electrical response was inverted as the sample was turned by 180° in the flow and null for perpendicular orientation, as expected from basic piezoelectricity principles. The electrical response varied consistently with nanowire distance to the tube outlet. Based on these results, we can expect that a matrix of such individually contacted nanowires can be used to map the amount and direction of a deformation or force distribution, with applications like gas or liquid flow sensing, fingerprint recognition or human-machine interfaces.

Before such a 2D mapping of force distribution could work properly, several technical issues need to be tackled: i) From a technological point of view, the fabrication process need to be optimized to obtain only individual NWs in the device surface. ii) An individual calibration of the contacted NWs is necessary to obtain the sensibility to a known lateral force or displacement, including a variation of the angle at which the force is applied; this could

possibly be done using AFM techniques or nano manipulators. iii) In order to improve the stability of the sensor and reduce its sensibility to gases, the NWs need to be encapsulated, for instance with a thin dielectric (polymer, oxide, etc.) [28]. Other interesting studies include tests under pure oxygen and a comparison with the measurements under air which could elucidate the effect of the adsorption of reactive oxygen species at the surface of ZnO NWs in this particular configuration. Further studies will concern these issues.

In this article we tested the mechanical sensor exploiting only the piezoelectric nature of the NW. Further studies on these devices will be made applying different bias voltages and measuring the current in function of the mechanical input.

Acknowledgements

The authors would like to thank Paulo Oliveira (Centro Federal de Educação Tecnológica de Minas Gerais, Brazil) for his help in the development of the characterization set-up. This work was performed using the clean-room facilities of the 'Plateforme Technologique Amont' in Grenoble, a member of the CNRS Renatech Network.

References

[1] K. Jenkins, V. Nguyen, R. Zhu, R. Yang, Sensors 15(9) (2015) 22914–22940.

[2] F.R. Fan, Feng Ru, W. Tang, and Z.L. Wang, Adv. Mater. 28(22) (2016) 4283–4305.

[3] Z.L. Wang, J. Phys. Chem. Lett. 1(9) (2010) 1388–1393.

[4] R. Yang, Y. Qin, L. Dai, Z.L. Wang, Nature Nanotech. 4(1) (2009) 34–39.

[5] S. Xu, Y. Qin, C. Xu, Y. Wei, R. Yang, Z.L. Wang, Nature Nanotech. 5(5) (2010) 366–373.

[6] Z.L. Wang, J. Song, Science 312(5771) (2006) 242–246.

[7] Z.L. Wang, Nano Today 5(6) (2010), 540–552.

[8] R. Hinchet, J. Ferreira, J. Keraudy, G. Ardila, E. Pauliac-Vaujour, M. Mouis, L. Montès, "Scaling rules of piezoelectric nanowires in view of sensor and energy harvester integration," in *IEDM IEEE International*, San Francisco, CA, USA, Dec. 2012, pp. 6.2.1–6.2.4.

[9] W. Wu, X. Wen, Z.L. Wang, Science 340(6135) (2013) 952–957.

[10] Y.S. Zhou, R. Hinchet, Y. Yang, G. Ardila, R. Songmuang, F. Zhang, Y. Zhang, W. Han, K. Pradel, L. Montès, M. Mouis, Adv. Mater. 25(6) (2013) 883-888.

[11] Z. Zhao, X. Pu, C. Han, C. Du, L. Li, C. Jiang, W. Hu, Z.L. Wang, ACS Nano 9 (2015) 8578.

[12] R. Agrawal, B. Peng, H.D. Espinosa, Nano Lett. 9(12) (2009) 4177–4183.

[13] R. Tao, G. Ardila, L. Montès, M. Mouis, Nano Energy 14 (2015) 62–76.

[14] R. Tao, M. Parmar, G. Ardila, P. Oliveira, D. Marques, L. Montès, M. Mouis, Semicond. Sci. Technol. 32 (2017) 064003 (10pp).

[15] G. Zhu, A.C. Wang, Y. Liu, Y. Zhou, Z.L. Wang, Nano Lett. 12(6) (2012) 3086–3090.

[16] S. Lee, R. Hinchet, Y. Lee, Y. Yang, Z.H. Lin, G. Ardila, L. Montès, M. Mouis, Z.L. Wang, Adv. Funct. Mater. 24(8) (2014) 1163–1168.

[17] X. Chen, J. Shao, N. An, X. Li, H. Tian, C. Xu, Y. Ding, J. Mater. Chem. C 3(45) (2015) 11806–11814.

[18] X. Xue, Y. Nie, B. He, L. Xing, Y. Zhang, Z.L. Wang, Nanotechn. 24(22) (2013) 225501.

[19] X. Wang, J. Song, J. Liu, Z.L. Wang, Science 316(5821) (2007) 102–105.

[20] S.N. Cha, J.S. Seo, S.M. Kim, H.J. Kim, Y.J. Park, S.W. Kim, J.M. Kim, Adv. Mater. 22(42) (2010) 4726–4730.

[21] W. Han, Y. Zhou, Y. Zhang, C.Y. Chen, L. Lin, X. Wang, S. Wang, Z.L. Wang, ACS Nano 6(5) (2012) 3760–3766.

[22] S. Lu, J. Qi, Z.L. Wang, P. Lin, S. Liu, Y. Zhang, RSC Advances 3(42) (2013) 19375–19379.

[23] X. Wang, J. Zhou, J. Song, J. Liu, N. Xu, Z.L. Wang, Nano lett. 6(12) (2006) 2768–2772.

[24] Z.L. Wang, Adv. Mater. 19(6) (2007) 889–892.

[25] E. Saoutieff, M. Allain, Y.R. Nowicki-Bringuier, A. Viana, E. Pauliac-Vaujour, Procedia Eng. 168 (2016) 1638–1641.

[26] B. Christian, J. Volk, I.E. Lukács, E. Sautieff, C. Sturm, A. Graillot, R. Dauksevicius, E. O'Reilly, O. Ambacher, V. Lebedev, Procedia Eng. 168 (2016) 1192–1195.

[27] E.A.L. Perez, E. Pauliac-Vaujour, M. Mouis, IEEE Trans. Nanotechnol. 15(3) (2016) 521–526.

[28] A. Bouvet-Marchand, A. Graillot, J. Volk, R. Dauksevicius, C. Sturm, M. Grundmann, E. Sautieff, A. Viana, B. Christian, V. Lebedev, J. Radó, I.E. Lukács, Q. Khánh N., D. Grosso, C. Loubat, J. Mater. Chem. C 6(3) (2018) 605–613.

[29] R. Yu, L. Dong, C. Pan, S. Niu, H. Liu, W. Liu, S. Chua, D. Chi, Z.L. Wang, Adv. Mater. 24(26) (2012) 3532-3537.

[30] Z. Zhang, K. Yao, Y. Liu, C. Jin, X. Liang, Q. Chen, L.M. Peng, Adv. Funct. Mater. 17(14) (2007) 2478-2489.

[31] J. Zhou, N.S. Xu, Z.L. Wang, Adv. Mater. 18(18) (2006) 2432–2435.

[32] Z. Li, R. Yang, M. Yu, F. Bai, C. Li, Z.L. Wang, J. Phys. Chem. C 112(51) (2008) 20114–20117.

[33] R. Tao, M. Mouis, G. Ardila, Adv. Electron. Mater. 4(1) (2018) 1700299.

[34] S. Kannan, M. Parmar R. Tao, G. Ardila, M. Mouis, 2016. J. Phys.: Conference Series (Vol. 773(1), p. 012071). IOP Publishing.

[35] D. Yang, Y. Qiu, Q. Jiang, Z. Guo, W. Song, J. Xu, Y. Zong, Q. Feng, X. Sun, Appl. Phys. Lett. 110(6) (2017) 063901.

[36] Y.H. Wang, C.P. Chen, C.M. Chang, C.P. Lin, C.H. Lin, L.M. Fu, C.Y. Lee, Microfluid. Nanofluid. 6(3) (2009): 333–346.

[37] R. Bao, C. Wang, L. Dong, R. Yu, K. Zhao, Z.L. Wang, C. Pan, Adv. Funct. Mater. 25(19) (2015) 2884–2891.

[38] S. Xu, Y. Wei, M. Kirkham, J. Liu, W. Mai, D. Davidovic, R.L. Snyder, Z.L. Wang, J. Am. Chem. Soc. 130(45) (2008) 14958–14959.

[39] V. Gaddam, R.R. Kumar, M. Parmar, M.M. Nayak, K. Rajanna, RSC Adv. 5(109) (2015) 89985–89992.

[40] P.S. Halasyamani, K.R. Poeppelmeier, Chem. Mater. 10(10) (1998) 2753–2769.

[41] V. Consonni, E. Sarigiannidou, E. Appert, A. Bocheux, S. Guillemin, F. Donatini, I. C. Robin, J. Kioseoglou, F. Robaut, ACS Nano 8(5) (2014) 4761–4770.

[42] M. Takata, D. Tsubone, H. Yanagida, J. Amer. Ceram. Soc. 59(1–2) (1976) 4–8.

[43] N.M. Kiasari, P. Servati, IEEE Electr. Device Lett. 32(7) (2011) 982–984.

[44] F. Morisot V. Nguyen, D. Muñoz-Rojas, M. Mouis, & C. Ternon, “Effect of passivation on two-dimensional randomly oriented ZnO nanowire networks for the electrical detection of acetone”, Nanowire Week 2018 Workshop, June 11-15, 2018 – Hamilton, Ontario, CANADA.

Figure Legends

Fig.1. Two configurations of individually contacted NWs on a sensor array: (a) NW with individual electrodes at its base and on top, after immersion into a polymer matrix (b) NW with two electrodes at its base (c) Operation mechanism of the individually contacted ZnO NWs as mechanical sensors. From FEM simulations the maximum piezoelectric potential under NW bending is generated at the bottom where the electrodes are placed.

Fig.2. Schematics of the pixel-controlled gas-flow sensor based on vertical piezoelectric ZnO NWs.

Fig.3. Schematics of the successive technological steps towards selective growth of ZnO NWs matrix by the hydrothermal method.

Fig.4. (a) SEM image of triangular-lattice/hexagonal-lattice patterned openings for selective growth of NWs for controlled NWs array density. (b-c) SEM images showing examples of localized growth on a patterned seed-layer

Fig.5. Top-view SEM images: (a) all 9 flow-sensing devices together in a single die; (b) general view of one device showing 20 metallic pads of 50 μm x 50 μm connected to metallic lines of 5 μm width; (c) enlargement on the central zone of the device where the 5 μm wide lines are connected to smaller pads of 5 μm x 5 μm. The latter are connected to narrower metallic lines of 250 nm width; (d) enlargement on the zone where two metallic lines are aligned with one mask opening for localized NW growth. (e) and (f) show different magnifications of one single-vertical NW with its 2 contacts.

Fig.6. (a) Schematic of the characterization conditions of individually contacted vertical NWs as mechanical sensors (b-c) Schematics top view and the cross-sectional view of the electrical configuration for the individual NW as a mechanical sensor, respectively.

Fig.7. Electrical response of a single ZnO NW (sample #2) in function of gas flow rate and kind of gas: (a) Variation in current with 20 sec period cycle for a fixed flow rate of 4 SLM (b)

Variation in the output current with respect to N2 gas-flow rate, and (c-d) sensor response with respect to flow rate in the case of compressed N2 gas and air, respectively.

Fig.8. Current variation in function of the orientation of the sample towards the gas tube outlet (a) with the gas-flow with normal orientation (from sample #2) and (b) with 180˚ change in the orientation (from sample #1) respectively (c) response of a single ZnO NW (sample #1) in function of flow rate and orientation (i.e. normal, reversed and perpendicular) towards the gas tube outlet.

Mitesh Parmar received his Ph.D. degree in 2012 from Indian Institute of Science, Bangalore, India. He is currently a Research fellow at International Iberian Nanotechnology Laboratory (INL), Braga, Portugal. Prior to this, his research experiences include tenures at South Korea (MEMS and Nanotechnology lab - National lab), India (IISc Banalore) and France (INP Grenoble - Minatec). He is also a lifetime member of Material Research Society of India (MRSI). His research is mainly focused on thin films, nanomaterials, design-development-testing of environmental/exhaust gas sensors using metal-oxides/composite-polymers as well as energy harvesters besides various application of piezoelectric materials, microfabrication and MEMS.

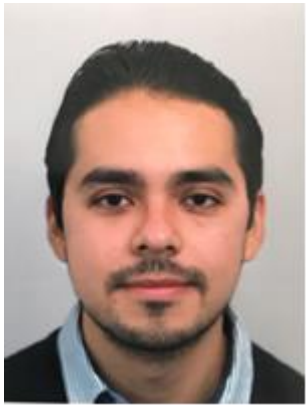

Edgar LEON PEREZ received the M.S. degree in Nanoscale Engineering from INSA Lyon-UCBL1-Ecole Centrale de Lyon (2012), and the Ph.D degree in Nanoelectronics and Nanotechnologies from University of Grenoble Alpes (2016), France.
During his Ph.D. he developed devices prefiguring a force/displacement sensor based on individually contacted vertical ZnO nanowires exploiting the piezotronic effect. In 2017, he conducted a postdoctoral training at Institute of Nanotechnologies of Lyon, France, concerning the use of indium oxide nanoparticles for non-volatile memory applications. Since 2018, he is with the STMicroelectronics Company, Crolles, France, where he is working in the development of CMOS imaging sensors.

Gustavo Ardila received his BS in electronic engineering and physics from the University of Andes, Colombia in 2002 and 2003, respectively, and his MS in microelectronic and microsystems circuit conception from the National Institute of Applied Science, Toulouse, France in 2004. He received his PhD degree in Electrical Engineering in 2008 from the Paul Sabatier University in Toulouse. After a postdoctoral position in LAAS-CNRS, in 2009 he became Associate Professor at the Grenoble Alpes University and researcher at IMEP-LAHC, Grenoble, France. His current research interests are MEMS and NEMS design, development and characterization, especially for mechanical energy harvesters and sensors.

Dr Elise Saoutieff (F) holds a PhD from the University of Belfort-Montbéliard (2010). Her thesis work has been made at EIFER (European Institute for Energy Research) in Karlsruhe, Germany, in the Solid Oxide Fuel Cell interconnectors field. She then joined the CEA-LITEN where she worked on the development of all solid-state-Lithium Microbatteries. She is working at CEA-LETI since 2014 and was involved in the FP7-ICT project PiezoMAT (CEA coordinator), which aim at design a new technology of high-resolution fingerprint sensor based on a matrix of inter-connected piezoelectric nanowires. She participates to Convergence-FlagEra (2017-2020) and InDeal-H2020 (2016-2019) projects.

Dr Emmanuelle Pauliac-Vaujour (F) obtained her PhD in nanotechnologies from the University of Nottingham, in 2008. She then took a post-doctoral position at CEA-Liten on the nano-engineering of new generations of fuel and solar cells. She joined CEA-Leti as permanent research staff in 2010, where her mission included developing innovative system solutions for nanotechnology integration. Since 2014, she has been entrusted with the lead of the Sensor Autonomy and Integration Laboratory at CEA-Leti, a lab specialized in IoT and connected objects and which develops embedded electronic systems and energy management solutions for both the industry and the general public.

Mireille MOUIS is coordinating research activities at IMEP-LAHC on new architectures for ultimate CMOS and on nanoscale devices that may extend performance and functionality of future integrated circuits. The group addresses device design and simulation as well as advanced electrical and near-field characterization. It has developed strong collaborations with academic, pre-industrial and industrial partners. Mireille Mouis has been participating or managing several research projects at the regional, national or European level. She has authored or co-authored more than 220 contributions in international conferences and refereed journals. She is serving as ED chapter chair for IEEE France section.